Active Class-C LC Phase Shifter with Automatic Amplitude Control

Meysam Sohani Darban, Fariborz Lohrabi Pour, Dong Sam Ha, Jeffrey Sean Walling
Bradley Department of Electrical and Computer Engineering,
Virginia Polytechnic Institute and State University, Blacksburg, VA, United States
{*meysam97, fariborzlp, ha, jswalling*}*@vt.edu*

***Abstract*—This paper introduces an automatic amplitude control (AAC) mechanism implemented on a class-C LC-based phase shifter. The AAC technique compensates for the amplitude attenuation of the phase shifter as a function of frequency and provides output swing control that enhances the suitability as a phase shifter in the auxiliary path of a load-modulated balanced power amplifier (LMB-PA). It can be utilized to calibrate and fine-tune the power amplifier (PA) performance after fabrication to achieve optimal performance. The circuit is designed and laid out using $22-\mathrm{nm}$ FD-SOI process technology. To demonstrate the proposed idea, the frequency of operation was chosen as 2.4 GHz. The total power consumption varies between $0.52-1$ mW due to phase control from $0-120^{\circ}$ with 0.085 dB amplitude error.**

***Index Terms*—Amplitude control, amplitude detector, LC tank, LMBA, phase shifter.**

I. Introduction

As wireless communications standards continue to evolve from 5G to 6G and beyond, the general goal is to increase wireless transmission capacity so that the network can achieve higher data rates. A direct means to achieving this goal is to use higher order modulation and/or Orthogonal Frequency Division Multiplexing (OFDM). Such modulations result in a signal with a high peak-to-average power ratio (PAPR) and require the power amplifier (PA) to be highly linear [1], [2]. Moreover, modern wireless signals use increasing bandwidth, particularly in next-G systems, to increase wireless data throughput further. The PA remains the dominant energy consumer in wireless systems, and because of that, PA efficiency is of paramount importance. It is increasingly accurate with newer standards seeking to use beamforming/multiple-input, multiple-output (MIMO) techniques that require arrayed transmitters. The efficiency of the PA is of paramount importance, particularly in phased arrays, due to excessive heat dissipation and energy consumption if the PA is inefficient.

The load-modulated balanced power amplifier (LMBPA) has recently been demonstrated as a suitable candidate for wideband and efficient operation [3], [4]. The block diagram schematic of an RF-LMBPA is shown in Fig. 1 [4]. The LMBPA consists of two paths. A balanced amplifier is on the main path. In the auxiliary path, a PA with input phase and amplitude control modulates the main path via the isolation port of the output quadrature hybrid power combiner. Load modulation via this path has been demonstrated to increase

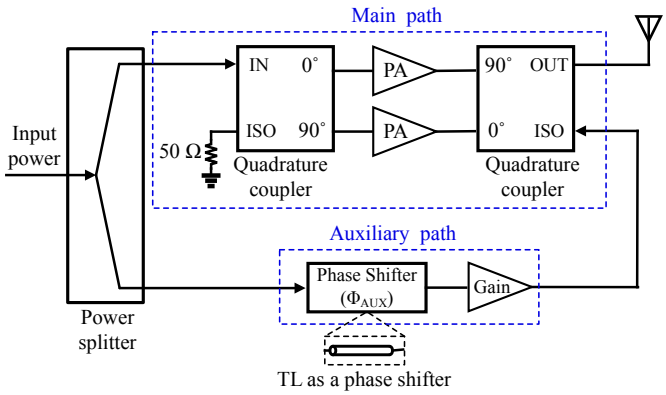

Fig. 1. Block diagram schematic of an LMBPA with a phase shifter in its auxiliary path (A transmission line can be used to create a fixed phase shift).

the efficiency of the PA, improve the PA linearity, and enhance the efficiency and linearity across frequencies [4]–[7].

Tunable load modulation can be used to enhance linearity, efficiency, or wideband performance, but in the initial RF-LMBPAs, the phase/amplitude weighting of the auxiliary path was fixed [4]. However, phase and amplitude control are preferred in the auxiliary path to achieve optimal performance after expected PVT variations in manufacturing or to provide reconfigurability. To overcome this issue, the fixed phase delay, typically created by a transmission line (TL) [8]–[10], is substituted for a variable phase shifter [11]. Hence, the system can be tuned and calibrated for the most suitable phase shift. Setting the Φ_{AUX} at its optimum value enhances the LMBA's performance after fabrication [12].

Adding a passive variable phase shifter, as in [9]–[11], can increase the area of the circuit. LC-phase shifters can be made more compact but are also subject to appreciable variation in amplitude as a function of phase shift. This amplitude variation can alter the performance, resulting in reduced linearity and efficiency [13]–[17]. Hence, this paper presents an automatic amplitude control (AAC) mechanism in a compact LC-based active phase shifter to compensate for amplitude variation at the output of the phase shifter. This paper is organized as follows. In Section II, the circuit concept and architecture of the proposed AAC mechanism are presented. This is followed in Section III with a prototype design and post-layout simulation results. Finally, conclusions and future results are presented in Section IV.

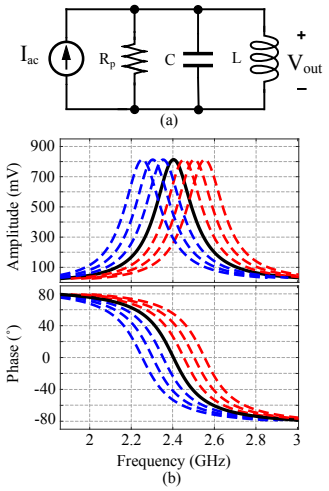

Fig. 2. (a) Circuit schematic of an LC-tank with finite Q, (b) Variation of amplitude and phase of V_{out} as a function of frequency, achieved by tuning the capacitor.

II. LC-Phase Shifter with Automatic Amplitude Control Concept

In this section, phase-shifting using an LC tank is first discussed, followed by the presented concept for an automatic amplitude control circuit.

A. Phase Variation in Resonant Circuits

Fig. 2 (a) shows a circuit model of a parallel LC resonant tank with a finite quality factor (Q). An AC current is injected into it with a constant amplitude. By sweeping the frequency of the injected current, the magnitude and phase of the output voltage (V_{out}) change, as shown in Fig. 2 (b). This is due to a second-order pole at the resonant frequency of the tank. By changing the frequency of resonance, a $\pm 90^{\circ}$ variation in the phase of V_{out} is achieved, centered on the resonant frequency, ω_0:

$$\omega_0 = \frac{1}{\sqrt{LC}}. \tag{1}$$

Hence, tuning of L or C can tune ω_0, as shown by the curves in Fig. 2 (b). Equation (2) shows the phase variation with respect to values of the passive network components and operation frequency.

$$\theta = \arctan\left(R_p\left(\frac{1 - LC\omega^2}{L\omega}\right)\right). \tag{2}$$

Using a varactor in place of the capacitor allows for the total capacitance of the circuit to be changed. If constant frequency is injected into the tank, based on (2), it provides a controllable phase shift at the tank's output.

B. LC-Based Phase Shifter

A conventional NMOS-only class-C differential amplifier is used to inject current into an LC tank, serving as its load, as shown in Fig. 3. Class-C operation provides high DC-RF efficiency for current injection, leading to reduced power consumption for the phase shifter. By tuning the capacitor, the

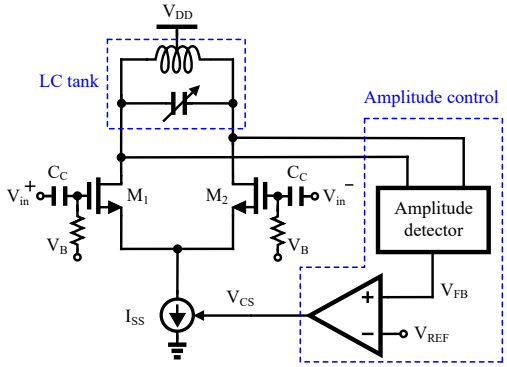

Fig. 3. Conceptual block diagram schematic of the LC-based phase shifter with automatic amplitude control.

phase of the output voltage across the tank can be adjusted as the resonant frequency is shifted, as discussed in Section II-A.

However, this is typically only usable over a relatively narrowband because the amplitude of the tank circuit also rolls off as the input frequency is changed to off-resonance. Though a significant phase shift can be achieved, the resulting signal amplitude becomes too small for an input signal frequency that is too far offset from the LC resonance. For low power consumption and to increase the phase change as a function of the offset frequency, the Q of the inductor should be increased as much as possible. However, higher Q also leads to increased attenuation for signals that are offset from the resonant frequency. One approach to solve this issue is to implement a limiting gain stage following the phase shifter to provide a rail-to-rail swing at its output. This approach suffers from two primary problems: *1)* A rail-to-rail buffer can consume significant power, particularly at high frequency. If a system needs more than one phase shift (e.g., to achieve a desired phase shift range or for MIMO operation), this approach increases the power consumption drastically. *2)* This method requires an additional variable gain amplifier or attenuator if precise output amplitude control is also needed.

Hence, the proposed solution is to use negative feedback to automatically adjust for the output amplitude variation as a function of the output phase shift. Such a scheme enables precisely controlling the signal's amplitude while not dramatically increasing power consumption. The proposed concept is shown in Fig. 3.

C. Automatic Amplitude Control

The proposed method uses an amplitude detection circuit that drives a comparison that automatically adjusts the tail current of the class-C amplifier to compensate for any losses that occur for phase shifts due to signals well off of the resonant frequency of the LC tank. To minimize power consumption, the detection and comparison circuits should be efficient. It is also noted that the power consumption of the system will vary as a function of the desired phase shift, as more current is used in the class-C amplifier for more significant phase variation.

The proposed amplitude detector circuit is shown in Fig. 4 and consists of an NMOS cross-coupled pair with a capacitor

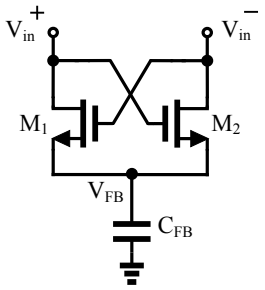

Fig. 4. Amplitude detector circuit.

(C_{FB}) in its tail. Applying a differential signal to this circuit charges the tail capacitor during each input half-cycle. The NMOS transistors should switch so that one turns on during each half period and charges C_{FB} to a value proportional to the detected amplitude. In each charging cycle, the enabled switch sees a portion of the swing applied as its gate-to-source voltage. The swing of the detector's input must be larger than the transistor's threshold voltage (V_{th}) to turn on entirely.

Leveraging a benefit of the IC technology, super low V_{th} NMOS transistors are chosen for this circuit. It should be noted that the circuit works without such devices; here, they are only used to improve the dynamic range, particularly for low signal amplitudes. V_{FB} has an average value that is proportional to the amplitude of the input. V_{FB} is a common-mode node of the differential pair; hence, it has ripples due to the second harmonic of the input signal. C_{FB} should be selected to be large enough to filter unwanted harmonics and decrease the ripple on V_{FB}.

The detector provides a DC signal that contains information about the output swing magnitude. This information is compared with a reference, and based on the comparison, the tail current injected into the tank is modified. The complete schematic of the proposed LC-based phase shifter with AAC is shown in Fig. 5. The outputs of the differential amplifier are directly connected to the detector circuit. Then, by implementing a low-power operational transconductance amplifier (OTA), the V_{FB} is compared with a reference DC voltage (V_{REF}). The output of the OTA provides a proportional voltage required by the class-C amplifier's current source, thus controlling the amount of current injected into the tank. The output can be precisely controlled to change the output swing using the value of V_{REF}, which could be set externally. Hence, variable amplitude control is also achievable.

The use of a feedback loop can lead to instability. Thus, the loop gain and bandwidth should be set to maintain stability and allow for reasonable settling time. In the presented work, the stability is primarily determined by the OTA compensation and C_{FB}. Both the OTA compensation and C_{FB} are selected to optimize settling/bandwidth tradeoffs. The loop gain is the product of the open-loop gain of the OTA and the transconductance of the tail current source. Increasing the loop gain reduces the error between V_{FB} and V_{REF}, which results in more precise amplitude control.

Although increasing the injection current results in increased power consumption, using class-C operation allows

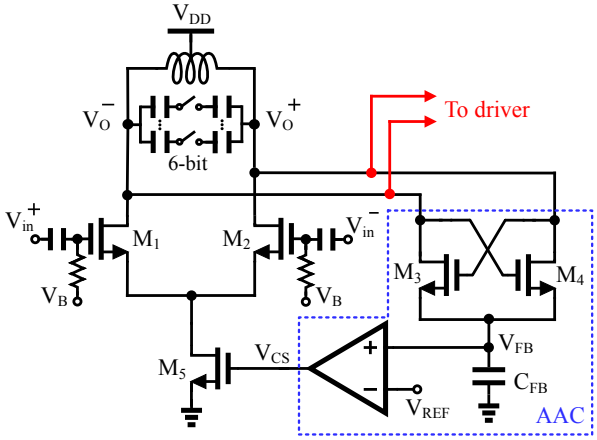

Fig. 5. Final schematic of the proposed phase shifter with AAC.

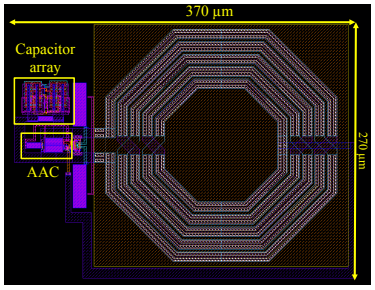

Fig. 6. Layout of the proposed circuit in 22-nm FD-SOI.

for improved efficiency, leading to a reduction in the overall current needed for swing compensation. The circuit's power consumption is adaptive to its operation condition and only consumes more power when needed. Simulation results verify that the maximum amplitude attenuation occurs when the phase variation is $> 45°$. In this range of operation, the magnitude of the LC tank impedance is small; hence, the phase sensitivity is reduced compared to the $0°$ point.

To enable a wide range of output phase variation, a large capacitance is needed, which can occupy a significant die area. Additionally, to maintain constant amplitude, more current should be injected into the tank, increasing power consumption. To avoid these issues, the phase shifter is constrained to operate with $\approx 0-90°$ of phase shift, covering one quadrant of operation. However, if larger phase shifts are desired, they can be achieved using a poly-phase filter [18]. Since the amplitude and phase of the output signal can be set to a desired value independently, the circuit can be used as a complex weight. At higher frequencies, this can be used in beamweighting in phased arrays or as a direct RF transmitter.

III. Post-Layout Simulation Results

The proposed circuit is customized to operate at 2.4 GHz. The phase shifter is laid out in 22-nm FD-SOI process technology and is extracted using Mentor Graphics Calibre extraction tools to consider parasitic effects due to interconnect and other metallization. The layout is shown in Fig. 6. The core area of the circuit is $370 \times 270 \mu m^2$ without considering pads. A low-

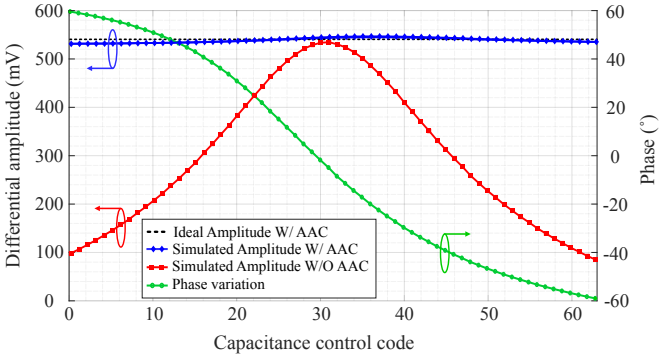

Fig. 7. Differential output amplitude compensation by adding the AAC mechanism and phase variation by changing the capacitance control code.

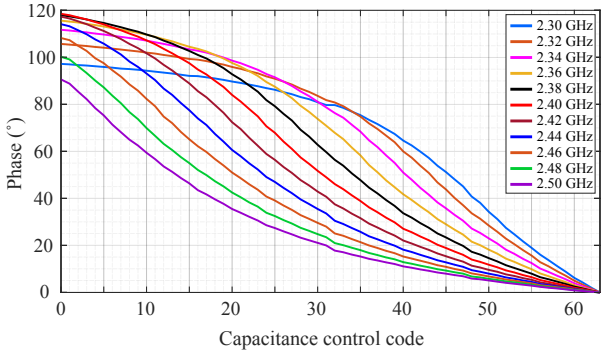

Fig. 8. Normalized phase variation over control codes at different input frequencies.

TABLE I
PERFORMANCE SUMMARY AND COMPARISON WITH STATE-OF-ART PHASE SHIFTERS

	This Work	[17]	[13]	[9]	[10]
Technology	**22-nm FD-SOI**	0.18 μm CMOS	65-nm CMOS	0.18 μm CMOS	0.5 μm GaAs
Architecture	**LC - Active**	RTPS	VM and VGA	Passive	Passive
frequency (GHz)	**2.4**	2.4	51 - 66	8 - 12	2.4
Phase Range (°)	**120**	120	360	360	360
RMS Amplitude Error (dB)	**0.085**	1	0.25 - 0.72	0.3	0.34
P_{DC} (mW)	**0.52 - 1**	111	5	0	0
Area (mm^2)	**0.1**	0.35	0.3	0.8	5.3

power OTA is designed for the AAC circuit that consumes 10μW. For the designed circuit, a 6-bit binary weighted array of MOM capacitors is implemented to enable $90°$ of phase variation in the output across all process corners. Fig. 7 shows the differential output amplitude compensation using the AAC mechanism. Based on the post-layout simulations, variations of the tank capacitor, applied by changing the capacitor array's control code, could reduce the output amplitude by $> 70\%$. However, enabling the AAC circuit keeps the output swing constant, as indicated in Fig. 7.

Based on corner simulations, the PVT variations only adjust the amplitude accuracy to less than 5% from the desired value. The root mean square (RMS) error for amplitude compensation from the ideal target value is 0.085 dB due to the high loop gain of the AAC system. Table I indicates the performance comparison with previous works. The proposed circuit is expected to have a better amplitude error owing to the high loop gain of the feedback mechanism. Additionally, compared to passive structures [9], [10], it consumes more power but occupies less die area.

In a full implementation, the phase shifter would connect to a PA via a driver, which would drive the input impedance of the PA. However, since this paper presents a standalone phase shifter, an open drain buffer is implemented to consider the effects of loading from a successive stage. The total power consumption of the phase shifter changes from 0.52–1 mW when delivering a constant 1 Vp-p amplitude across the nominal phase shift range. The power variation is due to the more significant current consumption required for larger

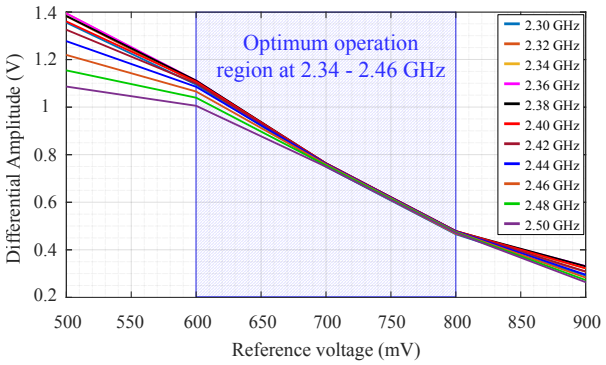

Fig. 9. Differential output amplitude variation by adjusting reference voltages at different input frequencies.

phase shifts. If accounting for the buffer, it consumes 1 mW. Based on the post-layout simulation results, the phase shifter can realize $\approx 0 - 120°$ phase shift, as shown in Fig. 7, which ensures covering at least $90°$ phase variation in all corners.

Fig. 8 indicates the normalized phase variation of the designed circuit by changing the capacitor array's input code over a frequency of 2.3–2.5 GHz. The ability to control the output amplitude by controlling V_{REF} is demonstrated in Fig. 9 over the same range of frequencies. The output differential amplitude varies from 0.3–1.4 V with constant phase across all phase control codes at 2.4 GHz. The linear range for V_{REF} is limited to between 600–800 mV, as lower voltage saturates the amplitude due to the tail current source operating in the triode. In contrast, higher voltages degrade the OTA and detector performance, leading to amplitude errors.

IV. Conclusion

A class-C LC-based active phase shifter with the AAC mechanism has been proposed to overcome the amplitude attenuation issue of the LC-based phase shifters. The circuit can be used for the load-modulated balanced amplifiers to optimize its performance after fabrication and improve back-off efficiency. The circuit is implemented in a 22-nm FD-SOI process technology that allows the system to work with 0.52–1 mW power consumption at 2.4 GHz while covering $120°$ of phase shift with constant, controllable amplitude with 0.085 dB RMS error.

REFERENCES

[1] S. Shakib, H.-C. Park, J. Dunworth, V. Aparin, and K. Entesari, "A highly efficient and linear power amplifier for 28-GHz 5G phased array radios in 28-nm CMOS," *IEEE Journal of Solid-State Circuits*, vol. 51, no. 12, pp. 3020–3036, 2016.

[2] L. Albasha, C. Clifton, Y. Jingu, A. Lawrenson, H. Motoyama, S. Bensmida, K. A. Morris, and K. Kohama, "An ultra-wideband digitally programmable power amplifier with efficiency enhancement for cellular and emerging wireless communication standards," *IEEE Transactions on Circuits and Systems I: Regular Papers*, vol. 63, no. 10, pp. 1579–1591, 2016.

[3] R. Quaglia and S. Cripps, "A load modulated balanced amplifier for telecom applications," *IEEE Transactions on Microwave Theory and Techniques*, vol. 66, no. 3, pp. 1328–1338, 2018.

[4] P. H. Pednekar, E. Berry, and T. W. Barton, "RF-input load modulated balanced amplifier with octave bandwidth," *IEEE Transactions on Microwave Theory and Techniques*, vol. 65, no. 12, pp. 5181–5191, 2017.

[5] J. Guo and K. Chen, "Reconfigurable hybrid asymmetrical load modulated balanced amplifier with high linearity, wide bandwidth, and load insensitivity," in *2023 IEEE/MTT-S International Microwave Symposium - IMS 2023*, 2023, pp. 462–465.

[6] X. A. Nghiem, J. Guan, and R. Negra, "Broadband sequential power amplifier with Doherty-type active load modulation," *IEEE Transactions on Microwave Theory and Techniques*, vol. 63, no. 9, pp. 2821–2832, 2015.

[7] Y. Cao and K. Chen, "Pseudo-Doherty load-modulated balanced amplifier with wide bandwidth and extended power back-off range," *IEEE Transactions on Microwave Theory and Techniques*, vol. 68, no. 7, pp. 3172–3183, 2020.

[8] P. Li, J. Niu, J. Fu, W. Chen, B. Lv, Z. Wang, and A. Li, "A novel 360° continuously tunable phase shifter based on varactor-loaded CRLH transmission line at exact 2.4 GHz," in *2016 IEEE International Conference on Electronic Information and Communication Technology (ICEICT)*, 2016, pp. 583–585.

[9] H. Alsuraisry, J.-H. Cheng, H.-W. Wang, J.-Y. Zhong, J.-H. Tsai, and T.-W. Huang, "A X-band digitally controlled 5-bit phase shifter in 0.18-μm CMOS technology," in *2015 Asia-Pacific Microwave Conference (APMC)*, vol. 2, 2015, pp. 1–3.

[10] X. Li, H. Fu, K. Ma, and J. Hu, "A 2.4–4 GHz wideband 7-bit phase shifter with low RMS phase/amplitude error in 0.5-μm GaAs technology," *IEEE Transactions on Microwave Theory and Techniques*, vol. 70, no. 2, pp. 1292–1301, 2022.

[11] V. Qunaj and P. Reynaert, "A Ka-band Doherty-like LMBA for high-speed wireless communication in 28-nm CMOS," *IEEE Journal of Solid-State Circuits*, vol. 56, no. 12, pp. 3694–3703, 2021.

[12] Y. Cao, H. Lyu, and K. Chen, "Load modulated balanced amplifier with reconfigurable phase control for extended dynamic range," in *2019 IEEE MTT-S International Microwave Symposium (IMS)*, 2019, pp. 1335–1338.

[13] G. H. Park, C. W. Byeon, and C. S. Park, "A 60-GHz low-power active phase shifter with impedance-invariant vector modulation in 65-nm CMOS," *IEEE Transactions on Microwave Theory and Techniques*, vol. 68, no. 12, pp. 5395–5407, 2020.

[14] S. Wang, J. Park, and S. Hong, "A K-band variable-gain phase shifter based on Gilbert-cell vector synthesizer with RC–RL poly-phase filter," *IEEE Microwave and Wireless Components Letters*, vol. 31, no. 4, pp. 393–396, 2021.

[15] C. So, E.-T. Sung, and S. Hong, "A 60-GHz variable-gain phase shifter with an active RL poly-phase filter," *IEEE Transactions on Microwave Theory and Techniques*, vol. 71, no. 2, pp. 593–601, 2023.

[16] X. Quan, X. Yi, C. C. Boon, K. Yang, C. Li, B. Liu, Z. Liang, and Y. Zhuang, "A 52–57 GHz 6-bit phase shifter with hybrid of passive and active structures," *IEEE Microwave and Wireless Components Letters*, vol. 28, no. 3, pp. 236–238, 2018.

[17] Y. Zheng and C. E. Saavedra, "An ultra-compact CMOS variable phase shifter for 2.4-GHz ISM applications," *IEEE Transactions on Microwave Theory and Techniques*, vol. 56, no. 6, pp. 1349–1354, 2008.

[18] M. Momeni and M. Moezzi, "A low loss and area efficient RC passive poly phase filter for monolithic GHz vector-sum circuits," *IEEE Transactions on Circuits and Systems II: Express Briefs*, vol. 66, no. 7, pp. 1134–1138, 2019.